

A possible solution of the puzzling variation of the orbital period of MXB 1659-298

R. Iaria,¹★ A. F. Gambino,¹ T. Di Salvo,¹ L. Burderi,² M. Matranga,¹
A. Riggio,² A. Sanna,² F. Scarano,² and A. D’Aì³

¹Dipartimento di Fisica e Chimica, Università di Palermo, via Archirafi 36 - 90123 Palermo, Italy

²Dipartimento di Fisica, Università degli Studi di Cagliari, SP Monserrato-Sestu, KM 0.7, Monserrato, 09042 Italy

³INAF/IASF Palermo, via Ugo La Malfa 153, I-90146 Palermo, Italy.

Accepted XXX. Received YYY; in original form ZZZ

ABSTRACT

MXB 1659-298 is a transient neutron star Low-Mass X-ray binary system that shows eclipses in the light curve with a periodicity of 7.1 hr. MXB 1659-298 turned on outburst in August 2015 after 14 years of quiescence. We span a baseline of 40 years using the eight eclipse arrival times present in literature and adding 51 eclipse arrival times collected during the last two outbursts.

We find that the companion star mass is $0.76 M_{\odot}$, the inclination angle of the system is $72^{\circ}.4$ and the corona surrounding the neutron star has a size of $R_c \simeq 3.5 \times 10^8$ cm. A simple quadratic ephemeris do not fit the delays associated with the eclipse arrival times, the addition of a sinusoidal term is needed. We infer a binary orbital period of $P = 7.1161099(3)$ hr and an orbital period derivative of $\dot{P} = -8.5(1.2) \times 10^{-12}$ s s⁻¹; the sinusoidal modulation has a period of 2.31 ± 0.02 yr. These results are consistent with a conservative mass transfer scenario during the outbursts and with a totally non-conservative mass transfer scenario during X-ray quiescence with the same mass transfer rate. The periodic modulation can be explained by either a gravitational quadrupole coupling due to variations of the oblateness of the companion star or with a presence of celestial body by orbiting around the binary system; in the latter case the mass of a third body is $M_3 = 21 \pm 2 M_J$.

Key words: X-rays: stars; X-rays: binaries; stars: neutron; binaries: eclipsing; ephemerides; stars: individual (MXB 1659-298)

1 INTRODUCTION

One of the most direct evidence for binary orbital motion is the presence of eclipse of the central source by a companion star. For Low Mass X-ray Binaries (LMXBs) with inclination angle between 75° and 80° the X-ray emission may be totally shielded by the companion star; when the companion transits between the X-ray central source and the observer the light curves show total eclipse. Because the total eclipse profile can be very well defined, the O-C method is usually applied to refine the orbital period or trace orbital period changes (see Chou 2014, for a recent review). To date, 12 LMXBs show total eclipses in their light curve; the best studied, because it was active for more than 20 years, is EXO 0748-676 (see Wolff et al. 2009, and references therein).

MXB 1659-298 is an eclipsing LMXBs. It was discovered by Lewin et al. (1976) in 1976, the authors observed X-ray type-I bursts in the light curve of the source, clear indication that the compact object hosted in the binary system is a neutron star. The source was observed in outburst up to 1978 with SAS3 and HEAO

(Cominsky et al. 1983; Cominsky & Wood 1984, 1989). The first detection of the presence of eclipses in the light curve of MXB 1659-298 was reported by Cominsky & Wood (1984), which estimated a periodicity of 7.1 hr. Cominsky & Wood (1989) analysed two whole eclipses estimating two eclipse arrival times. From 1978 up to 1999 the region of sky containing the MXB 1659-298 was monitored by the X-ray observatories onboard *Hakucho*, *EXOSAT* and *ROSAT*, but the source was never detected (see Cominsky & Wood 1989; Verbunt 2001). On April 1999 the Wide Field Cameras onboard *BeppoSAX* observed the source in outburst again (in ’t Zand et al. 1999). This new outburst continued up to September 2001. During the outburst MXB 1659-298 was observed with the Proportional Counter Array (PCA) onboard *Rossi X-ray Timing Explorer (RXTE)* by Wachter et al. (2000), with the Narrow Field Instruments (NFI) onboard *BeppoSAX* (Oosterbroek et al. 2001) and with *XMM-Newton*. From the analysis of the RXTE light curves of the source, Wachter et al. (2000) obtained four eclipse arrival times and found an orbital period derivative of MXB 1659-298 of $(-7.2 \pm 1.8) \times 10^{-11}$ s s⁻¹ suggesting that the orbit of the binary system is shrinking. Oosterbroek et al. (2001) obtained two eclipse arrival times from a *BeppoSAX*/NFI observation and com-

★ E-mail: rosario.iaria@unipa.it

binning their data with those present in literature found that the orbital period derivative, \dot{P}_{orb} , is positive with a value of $(7.4 \pm 2.0) \times 10^{-12}$ s/s. MXB 1659-298 turned on outburst on 2015 August 21 (Negoro et al. 2015) and it is still in outburst. Using data of the X-ray Telescope (XRT) onboard *Swift*, Bahramian et al. (2016) observed that the unabsorbed flux in the 0.5-10 keV energy range was 1.5×10^{-10} , 4.6×10^{-10} and 2.2×10^{-10} erg cm $^{-2}$ s $^{-1}$ on 2016 January 28, February 2 and 11, respectively.

Cominsky & Wood (1989) measured an eclipse duration, ΔT_{ecl} , of 932 ± 13 s and an ingress/egress duration of $\Delta T_{ing} = 41 \pm 13$ s and $\Delta T_{egr} = 19 \pm 13$ s, respectively. They showed that, if the companion star is a main-sequence star of $0.9 M_{\odot}$ with a temperature close to 5000 K, the scale height of the stellar atmosphere should be around 200 km and the authors concluded that the small value of the scale height cannot justify the large value of the measured ingress/egress durations. Furthermore, Cominsky & Wood suggested that the observed asymmetry between the ingress and egress duration could be caused by a one-sided extended corona of size 5×10^5 km.

From the analysis of four eclipses obtained with *RXTE*/PCA, Wachter et al. (2000) estimated an average eclipse duration of 901.9 ± 0.8 s and average values of ingress/egress durations of $\Delta T_{ing} = 9.1 \pm 3.0$ s and $\Delta T_{egr} = 9.5 \pm 3.3$ s. The authors discussed that the large spread of values associated with the ingress/egress times could be caused by flaring activity of the companion star or by the presence of an evaporating wind from the surface of the companion star caused by irradiation from the X-ray source.

Cominsky & Wood (1984) discussed the nature of the optical counterpart of MXB 1659-298, named V2134 Oph, assuming an orbital period of 7.1 hr and an eclipse duration of 900 s. They constrained the mass of the companion star to be between $0.3 M_{\odot}$ and $0.9 M_{\odot}$ for an inclination angle of the binary system of 90° and $71^{\circ}.5$, respectively. Warner (1995) inferred that the companion star mass is between 0.75 and $0.78 M_{\odot}$ if the companion fills its Roche lobe. This range of masses suggests that the companion is a K0 main-sequence star. During the quiescence of MXB 1659-298, Wachter et al. (2000) measured a magnitude in the *I*-band of 22.1 ± 0.3 mag and Filippenko et al. (1999) measured a magnitude in the *R*-band of 23.6 ± 0.4 mag. Wachter et al. found that the value of $(R - I)_0$ is compatible with an early K spectral type. Moreover, they suggested that, for a companion star belonging to the K0 class, the visual magnitude should be $V = 23.6$ mag, value that is compatible with the measured lower limit of $V > 23$ mag.

Galloway et al. (2008), analysing the type-I X-ray bursts observed with *RXTE*/PCA, inferred a distance to the source of 9 ± 2 and 12 ± 3 kpc for a hydrogen-rich and helium-rich companion star, respectively. Furthermore, Wijnands et al. (2001) detected nearly coherent oscillations with a frequency around 567 Hz during type-I X-ray bursts suggesting that the neutron star could be an X-ray millisecond pulsar with a spin period of 1.8 ms.

The interstellar hydrogen column density, N_H , was estimated by Cackett et al. (2008) during the X-ray quiescence of MXB 1659-298. They fitted the X-ray spectrum using *Chandra* and *XMM-Newton* data from the beginning of the quiescence in 2001 up to 2008 obtaining $N_H = (2.0 \pm 0.1) \times 10^{21}$ cm $^{-2}$. Two more recent *Chandra* observations of the source, taken in 2012 and analysed by Cackett et al. (2013), seem to suggest an increase of the interstellar hydrogen column density at the value of $(4.7 \pm 1.3) \times 10^{21}$ cm $^{-2}$. Cackett et al. (2013) proposed three different scenarios to explain the increase of N_H : a) material is building up in the outer region of the accretion disc, b) the presence of a precessing accretion disc,

and c) sporadic variability during quiescence due to low-level accretion.

Studying the *XMM-Newton* spectrum of MXB 1659-298, Sidoli et al. (2001) detected two absorption lines in the energy spectrum at 6.64 and 6.90 keV associated with the presence of highly ionised iron (Fe xxv and Fe xxvi ions) and absorption lines associated with highly ionised oxygen and neon (O viii 1s-2p, O viii 1s-3p, O viii 1s-4p and Ne ix 1s-2p transition) at 0.65, 0.77, 0.81 and 1.0 keV.

In this paper we report the updated ephemeris of MXB 1659-298 adding 45 eclipse arrival times obtained with *XMM-Newton* and *RXTE* during the outburst between 1999 and 2001 and six eclipse arrival times obtained with *XMM-Newton*, *NuSTAR* and *Swift*/XRT during the outburst started in 2015. The available temporal baseline allows to partially constrain the bizarre behaviour of the eclipse arrival times.

2 OBSERVATIONS

During the outburst occurred from 1999 to 2001, MXB 1659-298 was observed with *XMM-Newton* (Jansen et al. 2001) two times, the first time on March 22, 2000 and the second time on February 20, 2001. The second observation (obsid. 0008620701) was analysed by Sidoli et al. (2001) and Díaz Trigo et al. (2006), which studied the spectral properties of the source during the persistent emission, the dip and the eclipse; whilst the first observation (obsid. 0008620601) was never reported in literature. The PCA instrument onboard *RXTE* (Jahoda et al. 1996) observed several times the source from 1999 to 2001. In our analysis we selected 43 *RXTE*/PCA observations in which the eclipse is present and it is possible to estimate the ingress and egress time. The light curves of the discarded observations in which the eclipse is visible show the presence of type-I X-ray bursts either in ingress to or egress from the eclipses that does not allow us to obtain an accurate estimation of the eclipse arrival times.

The All Sky monitor (ASM, Levine et al. 1996) onboard *RXTE* monitored the 1999-2001 outburst (Fig. 1, left panel). The two *XMM-Newton* observations were performed at a similar ASM count rate of 2.5 c s $^{-1}$ (about 30 mCrab in flux), when the source reached the maximum flux. The outburst shows a sort of precursor lasting 100 d, after that the flux decreases up to a value compatible with zero for 86 d, and finally increases again rapidly reaching a constant flux of 30 mCrab for 700 d.

During the outburst started in 2015, MXB 1659-298 was observed once with *XMM-Newton* on September 26, 2015, two times with *NuSTAR* on September 28, 2015 and April 21, 2016 (see Harrison et al. 2013) and several snapshot observations were performed by *Swift*/XRT. No *Swift*/XRT observation shows an entire eclipse.

The Gas Slit Camera (GSC, Mihara et al. 2011) onboard the Monitor of All-sky X-ray Image (MAXI, Matsuoka et al. 2009) observed the recent outburst (see Fig. 1, right panel). The morphology of the outburst is similar to the previous one with a sort of precursor lasting 50 d, a new quiescent stage lasting 150 d and, after that, an increase of the flux at 30 mCrab lasting 150 d. The maximum GSC count rate is 0.12 c s $^{-1}$. *XMM-Newton* and *NuSTAR* (obsid. 90101013002) observed the source when the GSC count rate was 0.05 c s $^{-1}$; *NuSTAR* observed the source a second time when MXB 1659-298 was brighter with a corresponding GSC count rate of 0.1 c s $^{-1}$.

The European Photon Imaging Camera (Epic-pn, Strüder et al. 2001) onboard *XMM-Newton* collected data from the source in tim-

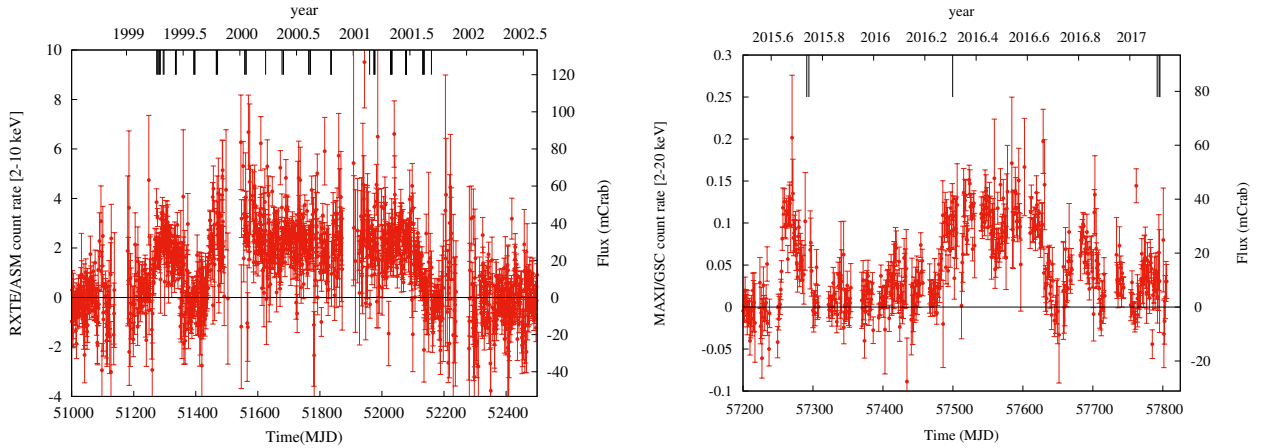


Figure 1. Light curve of MXB 1659-298 during the outburst occurred between 1999 and 2001 (left panel) and the latest started 2015 (right panel). The left panel shows the RXTE/ASM light curve in the 2-10 keV, the right panel shows the MAXI/GSC light curve in the 2-20 keV energy range; the bin time is one day for both the light curves. The eclipse arrival times are also indicated.

ing mode, with exposure times of 10, 32 and 34 ks, respectively. The *Epic-pn* light curve of the observation taken in 2001 shows two eclipses in the light curve (see Fig. 1 in [Sidoli et al.](#)). To verify the presence of eclipses in the *Epic-pn* light curves of the observations taken in 2000 and 2015 we filtered the source events with the Science Analysis System (SAS) ver. 15.0.0. We reprocessed the *Epic-pn* events and applied the solar-system barycentre corrections adopting as position of the source $RA = 255^\circ.527250$ and $Dec = -29^\circ.945583$ (see [Wijnands et al. 2003](#)). During the observation taken in 2000, the light curve of MXB 1659-298 shows an eclipse with a duration of 900 s approximately 1400 s after the start time. The count rate is 32 c s^{-1} and 1.4 c s^{-1} outside and during the eclipse, respectively. During the observation taken in 2015, the light curve shows the presence of a type-I X-ray burst at 12 ks from the start time. The count rate varies from 32 c s^{-1} at the beginning of the burst up to 320 c s^{-1} at the peak. An intense dipping activity is present at about 20 ks from the beginning of the observation, a complete eclipse is observed at 26 ks from the start time and an eclipse without the ingress is observed at beginning of the observation. The count rate out and during the eclipse is 32 and 1.4 c s^{-1} , respectively.

NuSTAR observed MXB 1659-298 two times in 2015 and 2016 with both the independent solid state photon counting detector modules (FPMA and FPMB), the elapsed times were 96 ks and 50 ks, respectively. We processed the raw (Level 1) data with the *ftool nupipeline* (Heasoft ver. 6.19), then obtaining cleaned and calibrated event data (Level 2). The solar-system barycentric corrected events of the FPMA and FPMB telescopes have been obtained applying the *tool nuproducts* on the Level 2 data. The corresponding light curves were obtained selecting a circular extraction region for the source events with a radius of $49''$ and using the 1.6-20 keV energy range. The persistent emission has a count rate of 2 c s^{-1} , at 90 ks from the start time a type-I X-ray burst is observed with a count rate at the peak of 160 c s^{-1} . A complete eclipse and an eclipse without the ingress are observed at 24 and 76 ks from the start time. The count rate during the eclipse is 0.02 c s^{-1} . It is also evident the presence of the ingress to the eclipse at 49.7 ks from the start time. During the second observation MXB 1659-298 is brighter, with a persistent count rate of 20 c s^{-1} and seven type-I X-ray bursts are present and a whole eclipse is observed at 30 ks from the start time of the observation. To increase the statistics of the *NuSTAR* light

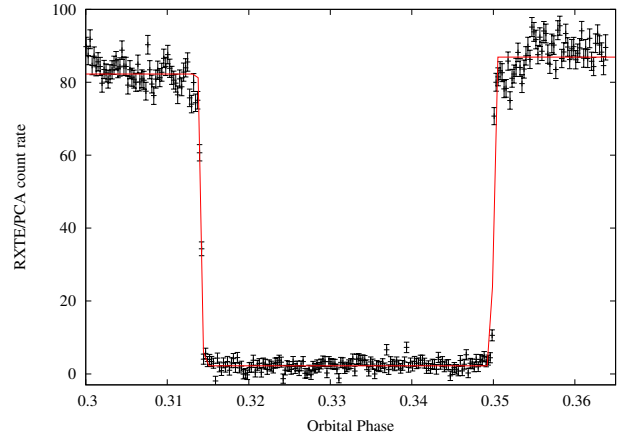


Figure 2. Eclipse of MXB 1659-628 observed by the RXTE/PCA instrument (observation P40050-04-16-00). The superimposed red function is the step-and-ramp function adopted to estimate the eclipse arrival time.

curve we summed the FPMA and FPMB light curve using the *ftool lcmath*.

To estimate the eclipse arrival times from the *RXTE/PCA* observations we analysed the standard product background-subtracted light curves with a bin time of 0.125 s and we applied the solar-system barycentric correction to the events using the *ftool faxbary*.

Finally, *Swift* ([Gehrels et al. 2004](#)) X-ray Telescope (XRT; [Burrows et al. 2005](#)) data were obtained as target of opportunity observations performed on February 8, 10 and 11, 2017 (obsid 0003400266, 0003400267 and 0003400268). All of the three observations cover the whole eclipse. The XRT data were processed with standard procedures (*xrtpipeline* v0.13.1), and with standard filtering and screening criteria with *ftools*. For our timing analysis, we also converted the event arrival times to the solar-system barycentre with the *tool barycorr* and subtracted the background using the *ftool lcmath*.

Table 1. Journal of the X-ray eclipse arrival times of MXB 1659-298

Point	Eclipse Time (MJD;TDB)	Cycle	Delay (s)	Ref.	Point	Eclipse Time (MJD;TDB)	Cycle	Delay (s)	Ref.
1	43 058.7260(2)	0	0(13)	[1],[2]	31	51 769.43726(2)	29378	107.0(1.3)	[4]
2	43 574.6441(2)	1740	26(13)	[1],[2]	32	51 835.261275(9)	29600	106.9(7)	[3]
3	51 273.978079(2)	27707	96.46(13)	[2]	33	51 836.447292(6)	29604	106.8(5)	[3]
4	51 274.571102(8)	27709	97.7(7)	[3]	34	51 837.040274(5)	29606	104.4(4)	[3]
5	51 277.832626(4)	27720	95.4(3)	[2]	35	51 960.08961(2)	30021	101(2)	[3]
6	51 278.425648(10)	27722	96.5(9)	[3]	36	51 974.321836(6)	30069	101.4(5)	[3]
7	51 281.687174(4)	27733	94.5(3)	[2]	37	51 974.914836(8)	30071	100.6(7)	[3]
8	51 283.762726(3)	27740	96.2(3)	[2]	38	51 976.397381(8)	30076	102.5(6)	[3]
9	51 285.838220(11)	27747	93.0(9)	[3]	39	51 977.286855(12)	30079	99.1(1.0)	[3]
10	51 295.029855(5)	27778	92.5(4)	[3]	40	52 027.692627(9)	30249	99.2(7)	[3]
11	51 297.698476(8)	27787	99.4(7)	[3]	41	52 029.768118(8)	30256	95.8(7)	[3]
12	51 334.464970(12)	27911	93.6(1.1)	[3]	42	52 030.954185(12)	30260	100.0(1.1)	[3]
13	51 335.650973(6)	27915	92.2(5)	[3]	43	52 032.733167(8)	30266	96.1(7)	[3]
14	51 337.133479(6)	27920	90.8(5)	[3]	44	52 076.615786(4)	30414	91.7(3)	[3]
15	51 393.46935(4)	28110	92(4)	[3]	45	52 077.208801(7)	30416	92.2(6)	[3]
16	51 396.13784(4)	28119	87(3)	[3]	46	52 077.801847(6)	30418	95.3(5)	[3]
17	51 397.32378(3)	28123	81(3)	[3]	47	52 078.394837(7)	30420	93.7(6)	[3]
18	51 466.112958(9)	28355	91.5(8)	[3]	48	52 078.987831(8)	30422	92.4(7)	[3]
19	51 467.29898(12)	28359	92.2(1.0)	[3]	49	52 131.469068(10)	30599	86.8(9)	[3]
20	51 470.264016(9)	28369	91.1(8)	[3]	50	52 132.65509(2)	30603	87(2)	[3]
21	51 557.436333(6)	28663	89.8(5)	[3]	51	52 133.24811(8)	30605	88(7)	[3]
22	51 561.290937(6)	28676	93.7(5)	[3]	52	52 136.50958(8)	30616	81(7)	[3]
23	51 562.477008(6)	28680	98.3(5)	[3]	53	52 159.34046(2)	30693	83.9(1.4)	[3]
24	51 625.03951(2)	28891	104(2)	[3]	54	57 291.24010(2)	48001	17(2)	[3]
25	51 677.817305(4)	29069	101.3(4)	[3]	55	57 294.20513(2)	48011	16(2)	[3]
26	51 681.671901(6)	29082	104.5(5)	[3]	56	57 499.682737(14)	48704	13.7(1.2)	[3]
27	51 682.857903(7)	29086	103.2(6)	[3]	57	57 792.03631(3)	49690	23(3)	[3]
28	51 763.803676(5)	29359	106.3(4)	[3]	58	57 794.70484(5)	49699	22(4)	[3]
29	51 764.989711(8)	29363	107.7(7)	[3]	59	57 795.89087 (5)	49703	23(4)	[3]
30	51 768.84426(2)	29376	106.0(1.4)	[4]					

NOTE — Epoch of reference 43 058.72595 MJD, orbital period 7.11610872 hr, the associated errors are at 68% confidence levels; [1] [Cominsky & Wood \(1989\)](#), [2] [Wachter et al. \(2000\)](#), [3] this work, [4] [Oosterbroek et al. \(2001\)](#).

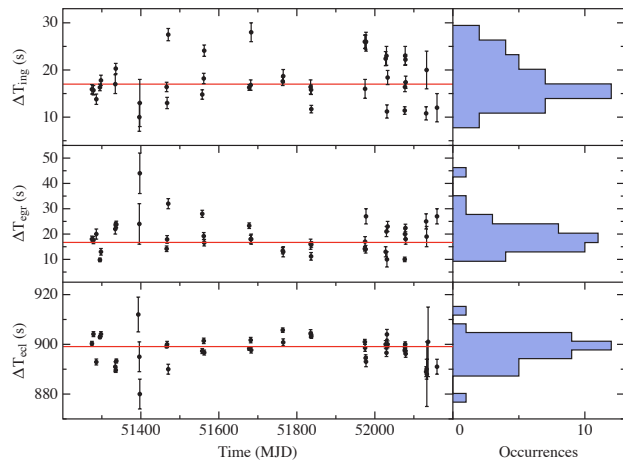


Figure 3. From the top-left to the bottom-left the ingress, egress and eclipse duration, respectively, as function of time. The values are obtained from the RXTE/PCA eclipses analysed in this work. The red lines indicate the average values for each duration. From the top-right to the bottom-right we show the histograms of the occurrences of the ingress, egress and eclipse duration.

3 METHOD AND ANALYSIS

To estimate the eclipse arrival times, we folded the solar-system barycentric corrected light curves using a trial time of reference and orbital period, T_{fold} and P_0 , respectively. The value of the adopted T_{fold} corresponds to a time close to the start time of the corresponding observation. The adopted value of P_0 is 7.11610872 hr corresponds to the value of the orbital period at $T_0 = 43\,058.72609$ MJD obtained by [Oosterbroek et al. \(2001\)](#) adopting quadratic ephemeris.

We fitted the eclipse profiles with a simple model consisting of a step-and-ramp function, where the count rates before, during, and after the eclipse are constant and the intensity changes linearly during the eclipse transitions. This model involves seven parameters: the count rate before, during, and after the eclipse, called C_1 , C_2 , and C_3 , respectively; the phases of the start and stop times of the ingress (ϕ_1 and ϕ_2), and, finally, the phases of the start and stop times of the egress (ϕ_3 and ϕ_4). We show a typical eclipse of MXB 1659-298 in Fig. 2. The eclipse was observed during the RXTE/PCA observation P40050-04-16-00, the superimposed red function is the step-and-ramp best-fitting function. The phase corresponding to the eclipse arrival time ϕ_{ecl} is estimated as $\phi_{ecl} = (\phi_2 + \phi_3)/2$. The corresponding eclipse arrival time is given by $T_{ecl} = T_{fold} + \phi_{ecl}P_0$. To be more conservative, we scaled the error associated with ϕ_{ecl} by the factor $\sqrt{\chi^2_{red}}$ to take into account values of χ^2_{red} of the best-fit

Table 2. Best-fit values

Parameter	LQ	LQS	LQCS
a (s)	-109 ± 38	65 ± 20	9 ± 29
b (s d ⁻¹)	0.046 ± 0.007	0.015 ± 0.004	0.037 ± 0.009
c (×10 ⁻⁶ s d ⁻²)	-2.6 ± 0.3	-1.2 ± 0.2	-4.0 ± 1.1
d (×10 ⁻¹⁰ s d ⁻³)	-	-	1.0 ± 0.4
A (s)	-	9.6 ± 0.6	10.2 ± 0.7
P _{mod} (d)	-	843 ± 7	855 ± 8
t _φ (d)	-	137 ± 75	-7 ± 82
χ ² (d.o.f.)	4083(56)	512(53)	455(52)

model larger than one. We show the obtained eclipse arrival times in Barycentric Dynamical Time (TDB), in units of MJD, in Tab. 1.

We used the 43 RXTE/PCA observations to estimate the average duration, ΔT_{ecl} , ΔT_{ing} and ΔT_{egr} of the eclipse, the ingress and the egress, respectively. The values of ΔT_{ecl} , ΔT_{ing} and ΔT_{egr} for each eclipse are shown as function of the eclipse arrival times in Fig. 3. We found that ΔT_{ecl} is scattered between 890 and 910 s. Fitting the values of eclipse duration with a constant we obtained a χ^2 (d.o.f.) of 561(42) and a best-fit value of $\Delta T_{ecl} = 899.1 \pm 0.6$ s at 68% confidence level (c.l.). The ingress duration is scattered between 10 and 30 s while the egress duration is scattered between 10 and 35 s. Fitting the ingress duration values with a constant we obtained a χ^2 (d.o.f.) of 457(38) and a best-fit value of $\Delta T_{ing} = 17.0 \pm 0.7$ s at 68% c. l., while, fitting the egress duration values we obtained a χ^2 (d.o.f.) of 560(39) and a best-fit value of $\Delta T_{egr} = 16.7 \pm 0.9$ s at 68% c. l. The associated errors were scaled by the factor $\sqrt{\chi^2_{red}}$ to take a value of χ^2_{red} of the best-fit model larger than one into account. We find that the average duration of the ingress and egress are similar. We also show in Fig. 3 the occurrences of the measured ingress, egress and duration using a bin of 3.1, 3.7 and 3.5 s, respectively.

We calculated the delays with respect to $P_0 = 7.11610872$ hr and to a reference epoch of $T_0 = 43\,058.72595$ MJD, corresponding to the first eclipse arrival time obtained by Cominsky & Wood (1989). The inferred delays, in units of seconds, of the eclipse arrival times with respect to a constant orbital period are reported in Tab. 1. For each point we computed the corresponding cycle and the eclipse arrival time in days with respect to the adopted T_0 . We show the delays vs. time in Fig. 4 (top panel).

Initially we fitted the delays with a quadratic function

$$y(t) = a + bt + ct^2, \quad (1)$$

where t is the time in days (MJD-43 058.72595), $a = \Delta T_0$ is the correction to T_0 in units of seconds, $b = \Delta P/P_0$ in units of s d⁻¹ with ΔP the correction to the orbital period, and finally, $c = 1/2 \dot{P}/P_0$ in units of s d⁻², with \dot{P} representing the orbital period derivative. The quadratic function does not give an acceptable fit to the data, χ^2 (d.o.f.) of 4083(56), the best-fit parameters are shown in the second column of Tab. 2. Since the delays seem to show a periodic modulation we fitted them using the function

$$y(t) = a + bt + ct^2 + A \sin \left[\frac{2\pi}{P_{mod}}(t - t_\phi) \right], \quad (2)$$

where A is the amplitude of the sinusoidal function in seconds, P_{mod} is the period of the sine function in days, and, finally, t_ϕ is the time in days at which the sinusoidal function is null. In this case we obtained a value of χ^2 (d.o.f.) of 512(53), by adding the sinusoidal term we find a F-test probability chance improvement of 7×10^{-24}

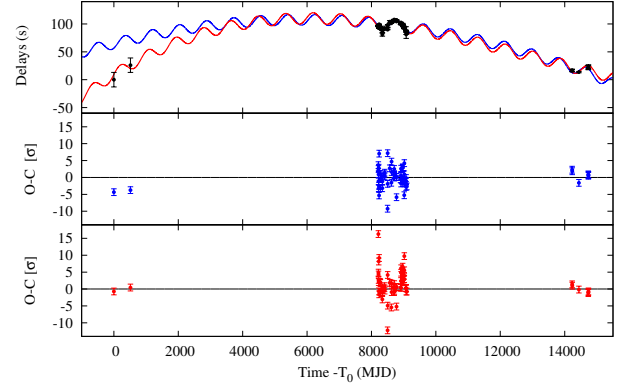


Figure 4. Top panel: delays with respect to the predicted eclipse arrival times, assuming as epoch of reference $T_0 = 43\,058.72595$ MJD and as orbital period $P_0 = 7.11610872$ hr, plotted versus time. The blue and red curves indicate the best-fit functions corresponding to eqs. 2 and 4, respectively. Middle panel: residuals in units of σ with respect to the blue curve. Bottom panel: residuals in units of σ with respect to the red curve.

suggesting that the presence of the periodic modulation is statistically significant. The best-fit function, indicated with a blue curve, and the corresponding residuals are shown in the top and middle panels of Fig. 4. The best-fit values are shown in the third column of Tab. 2. The corresponding ephemeris (hereafter LQS) is

$$T_{ecl}(N) = \text{MJD(TDB)}\,43\,058.7267(2) + 0.296504580(13)N - 1.3(2) \times 10^{-12}N^2 + A \sin \left[\frac{2\pi}{N_{mod}}N - \phi \right], \quad (3)$$

where N indicates the number of cycles, $N_{mod} = P_{mod}/P_0$ and $\phi = 2\pi t_\phi/P_{mod}$. We find that the orbital period derivative is $\dot{P} = -8.5(1.2) \times 10^{-12}$ s s⁻¹, the sinusoidal modulation has a period of $P_{mod} = 2.31 \pm 0.02$ yr and a semiamplitude of $A = 9.6 \pm 0.6$ s.

It is evident that the LQS ephemeris does not predict the first two eclipse arrival times. A possible explanation is that the orbital period derivative is changing from 1976 up to now. To take into account of that we added a cubic term to eq. 2, the function become

$$y(t) = a + bt + ct^2 + dt^3 + A \sin \left[\frac{2\pi}{P_{mod}}(t - t_\phi) \right], \quad (4)$$

where d includes the presence of a derivative of \dot{P} with $d \approx \ddot{P}/(6P)$. We obtain a value of χ^2 (d.o.f.) of 455(52) by fitting the delays with the function of eq. 4; by adding the cubic term we find a F-test probability chance improvement of 0.014 indicating that the improvement of the fit is between two and three σ of confidence level. The best-fit function, indicated with a red curve, and the corresponding residuals are shown in the top and bottom panel of Fig. 4. The best-fit values are shown in the fourth column of Tab. 2. The corresponding ephemeris (hereafter LQCS) is

$$T_{ecl}(N) = \text{MJD(TDB)}\,43\,058.7261(3) + 0.296504566(3)N - 4.0(1.1) \times 10^{-12}N^2 + 3.0(1.2) \times 10^{-17}N^3 + A \sin \left[\frac{2\pi}{N_{mod}}N - \phi \right], \quad (5)$$

We find that the orbital period derivative at time $T_0 = 43\,058.7261$ MJD is $\dot{P} = -2.7(7) \times 10^{-11}$ s s⁻¹ and the orbital period second

derivative is $\dot{P} = 2.4(9) \times 10^{-20} \text{ s s}^{-2}$. The sinusoidal modulation has a period of $P_{\text{mod}} = 2.34 \pm 0.02 \text{ yr}$ and a semi-amplitude of $A = 10.2 \pm 0.7 \text{ s}$.

4 DISCUSSION

We have analysed the eclipse arrival times of MXB 1659-298 to estimate its ephemeris. Our baseline spans 40 years and covers the three outburst of the source observed from 1976 up to date. We have added 51 eclipse arrival times, corresponding to the outbursts occurred in 1999-2001 and in 2015-2017, to the data reported in literature. The campaign of observations made with *Rossi-XTE/PCA* during the outburst in 1999-2001 has allowed us to find a clear periodical modulation of 2.3 years that is confirmed by the six eclipse arrival times obtained during the recent outburst. We find that the LQS ephemeris predict the eclipse arrival times except for the two eclipses observed in 1976-1978. The addition of a cubic term (LQCS ephemeris) allows to predict all the available ephemeris, however the statistical improvement is less than three sigma suggesting that a larger baseline is needed to confirm the more complex ephemeris. In the following we discuss the LQS ephemeris.

To estimate the eclipse arrival times we fitted the shape of the eclipse using a step-and-ramp function. We used the *RXTE/PCA* observations, covering 2.4 years during the second outburst of MXB 1659-298, to estimate the ingress/egress and eclipse durations. The obtained values are scattered, the mean values associated with the eclipse, ingress and egress are $\Delta T_{\text{ecl}} = 899.1 \pm 0.6 \text{ s}$, $\Delta T_{\text{ing}} = 17.0 \pm 0.7 \text{ s}$ and $\Delta T_{\text{egr}} = 16.7 \pm 0.9 \text{ s}$ with the errors at one σ , respectively. We find that the ingress and egress durations are similar contrarily to what reported by Cominsky & Wood (1989), that obtained an ingress and egress duration of $41 \pm 13 \text{ s}$ and $19 \pm 13 \text{ s}$, respectively. Our different results can be explained by the larger sample and the higher quality dataset.

The ingress, egress, and eclipse durations show a jittered behaviour of the order of 15 s as similarly observed in EXO 0748-676 (Wolff et al. 2002). Wolff et al. (2007) discussed the possibility that magnetic activity of the companion star generates extended coronal loops above the photosphere that could explain the amplitude of the observed jitter. This scenario may be plausible because the companion star in EXO 0748-676 has a mass of $0.4 M_{\odot}$ and it is associated with a late K or early M type main-sequence star. Such stars can have magnetic activity if they rotate and if they have significant convective envelopes (see Wolff et al. 2007). The companion star in MXB 1659-298 is an early K type main-sequence star (see below), and hence it may have similar magnetic activity. Instead, Ponti et al. (2017) showed that AX J1745.6-2901 has a different phenomenology; although jitters are observed in the ingress and egress, the eclipse duration is nearly constant. Ponti et al. suggested that the matter ejected from the accretion disc could reach the companion star with a ram pressure comparable to the pressure in the upper layers of the companion star (that is a K type main-sequence star). This interaction could displace the atmosphere of the companion star delaying both the ingress and egress time.

We can estimate the companion star mass from the size of its Roche lobe. The Roche lobe radius R_{L_2} of the companion star in MXB 1659-298 can be expressed by using the formula of Paczyński (1971)

$$R_{L_2} = 0.462a \left(\frac{m_2}{m_1 + m_2} \right)^{1/3}, \quad (6)$$

where a is the orbital separation of the binary system and m_1 is

the neutron star mass in units of solar masses. Combining the previous equation with the third Kepler's law we find that $R_{L_2} = 0.233 m_2^{1/3} P_h^{2/3} R_{\odot}$. Assuming that the companion star fills its Roche lobe then the radius of the companion star R_2 coincides with R_{L_2} . We can estimate the mass of the companion star knowing its mass-radius relation, under the hypothesis it is in thermal equilibrium. Using the empirical mass-radius relation $R_2/R_{\odot} = (M_2/M_{\odot})^{0.88} = m_2^{0.88}$ valid for m_2 lower than $0.8 M_{\odot}$ (see Patterson 1984, eq. 3) we find that the companion star should have a mass of $0.76 M_{\odot}$ and a radius of $0.79 R_{\odot}$.

Using *RXTE/PCA* data, Galloway et al. (2008) observed that the maximum flux of MXB 1659-298 during the outburst occurred in 1999 is $\sim 1.0 \times 10^{-9} \text{ erg s}^{-1} \text{ cm}^{-2}$ in the 2-25 keV energy range. During the outburst occurred in 2015 the maximum count rate measured with MAXI/GSC in the 2-20 keV energy band is 0.12 c s^{-1} (see Fig. 1, right panel), that corresponds to a flux of $1.1 \times 10^{-9} \text{ erg s}^{-1} \text{ cm}^{-2}$, compatible with the maximum flux observed by *RXTE/PCA* during the outburst in 1999. To estimate the flux in the 0.1-100 keV energy band, we adopted the best-fit model of the persistent spectrum obtained by Sidoli et al. 2001, from which we extrapolate an unabsorbed flux of $1.3 \times 10^{-9} \text{ erg s}^{-1} \text{ cm}^{-2}$.

From the analysis of the type-I X-ray bursts the distance to MXB 1659-298 was estimated to be 9 ± 2 and $12 \pm 3 \text{ kpc}$ for a hydrogen-rich and helium-rich companion star, respectively (see Galloway et al. 2008). Assuming a neutron star mass of $1.4 M_{\odot}$ and a neutron star radius of 10 km we find that the mass accretion rate associated with the maximum luminosity during outbursts is $1.1^{+0.6}_{-0.4} \times 10^{-9} M_{\odot} \text{ yr}^{-1}$ for a distance of $9 \pm 2 \text{ kpc}$.

We have obtained an estimate of the orbital period derivative, $\dot{P} = -8.5(1.2) \times 10^{-12} \text{ s s}^{-1}$ and we show that it is possible to explain this result assuming that during the outbursts the mass-transfer is conservative while during the X-ray quiescence the mass transfer is totally non-conservative with the same mass transfer rate. We assume that the mass transfer rate, during both outbursts and quiescence, corresponds to the mass accretion rate observed at the peak of the outburst ($1.1^{+0.6}_{-0.4} \times 10^{-9} M_{\odot} \text{ yr}^{-1}$). We estimate that the total duration of the outbursts corresponds to only 10% of the whole timespan. Defining β as $\dot{M}_1 = -\beta \dot{M}_2$ we have that $\beta \approx 0.1$.

Furthermore, we assume that the matter provided by the companion star is ejected from the binary system during the quiescence. The specific angular momentum, l_{ej} , with which the transferred mass is lost from the system can be written in units of the specific angular momentum of the secondary, that is $\alpha = l_{ej}/(\Omega_{\text{orb}} r_2^2) = l_{ej} P (M_1 + M_2)^2 / (2\pi a^2 M_1^2)$, where r_2 is the distance of the secondary star from the centre of mass of the system, a is the orbital separation and P is the orbital period of the binary system. We assume that the matter leaves the system with the specific angular momentum of the inner Lagrangian point. Since the companion star mass and neutron star mass are $0.76 M_{\odot}$ and $1.4 M_{\odot}$, respectively, we infer that $\alpha \approx 0.282$.

The secular mass transfer rate can be expressed as

$$\dot{m}_{-8} = -0.6 m_1^{8/3} P_{2h}^{-8/3} q^2 (1+q)^{-1/3} h(\alpha, \beta, q, n)^{-1} [1 + T_{MB}], \quad (7)$$

where P_{2h} is the orbital period in units of two hours, q is the ratio m_2/m_1 , \dot{m}_{-8} is the mass transfer rate in units of $10^{-8} M_{\odot} \text{ yr}^{-1}$ and T_{MB} is the term that takes into account of the angular momentum of the system lost via magnetic braking. The function $h(\alpha, \beta, q, n)$ is defined as

$$h(\alpha, \beta, q, n) = 3 \left[1 - \beta q - \frac{1 - \beta}{1 + q} \left(\frac{q}{3} + \alpha \right) \right] - \frac{1 - 3n}{2} \quad (8)$$

(see Di Salvo et al. 2008; Burderi et al. 2009, 2010), where n is the mass-radius index adopted above. The term T_{MB} is

$$T_{MB} = 8.4(k^2)_{0.1} f^{-2} m_1^{-1} P_{2h}^2 q^{1/3} (1+q)^{2/3} \quad (9)$$

(Burderi et al. 2010), where f is a dimensionless parameter which assumes the value of 1.78 (Smith 1979) and k is the radius of gyration of the star; we assume $k = 0.277$ which is the appropriate value for a $1 M_\odot$ ZAMS star (Claret & Gimenez 1989). Using the orbital period obtained from the LQS ephemeris we find that absolute value of the secular mass transfer rate is $\dot{m} \approx 9.4 \times 10^{-10} M_\odot \text{ yr}^{-1}$. This value is compatible with the mass accretion rate at the peak of the outburst that is $1.1^{+0.6}_{-0.4} \times 10^{-9} M_\odot \text{ yr}^{-1}$ for a distance to the source of 9 ± 2 kpc.

The secular orbital period derivative is given by

$$\dot{P}_{-12} = 1.37q(1+q)^{-1/3} m_1^{5/3} P_{2h}^{-5/3} \left[\frac{1/3 - n}{2g(\alpha, \beta, q) - 1/3 + n} \right] \times [1 + T_{MB}], \quad (10)$$

where

$$g(\alpha, \beta, q) = 1 - \beta q - \frac{1 - \beta}{1 + q} \left(\frac{q}{3} + \alpha \right) \quad (11)$$

(see Di Salvo et al. 2008; Burderi et al. 2009, 2010). Substituting the values in eq. 10 we find that the secular orbital period derivative is $-1.0 \times 10^{-11} \text{ s s}^{-1}$ which is compatible at one sigma with the value of $\dot{P} = -8.5(1.2) \times 10^{-12} \text{ s s}^{-1}$ inferred from the eclipse arrival times.

During quiescence, a highly non-conservative mass transfer in this source may be justified by the fact that MXB 1659-298 is a fast spinning neutron star. In fact, nearly coherent pulsations at 1.8 msec have been detected in this source during type-I burst (Wijnands et al. 2001). During quiescent periods, if the region around the neutron star is free from matter up to the light cylinder radius, the radiation pressure of the rotating magnetic dipole, given by the Larmor formula, may be able to eject from the system the matter transferred by the companion star directly at the inner Lagrangian point, according to the mechanism named *radio ejection* and described in detail in Burderi et al. (2001). This mechanism has been invoked to explain the high orbital period derivative observed in the accreting millisecond pulsar (AMSP) SAX J1808.4-3658 (see Di Salvo et al. 2008; Burderi et al. 2009), and, more recently, for the AMSP SAX J1748.9-2021 for which a high orbital period derivative is also observed (Sanna et al. 2016). We therefore suggest that a similar mechanism is also working for MXB 1659-298.

The *radio ejection* mechanism might also explain the changes of the equivalent hydrogen column observed during quiescence by Cackett et al. (2008, 2013). The matter provided by the companion is ejected from the inner Lagrangian point forming a circumbinary ring of matter around MXB 1659-298 located in the equatorial plane. Because of the large inclination angle of the system it is possible that the ejected matter interposes between the source and the observer; local density inhomogeneities and/or changes in the mass transfer rate could produce changes in the equivalent hydrogen column. We use the eq. 4 of Iaria et al. (2013) to estimate the density of the ejected matter

$$n(r) \approx 6.9 \times 10^{11} (1 - \beta) \zeta^{-1} \eta^{-1} \dot{m}_E (m_1 + m_2)^{-1} P_h^{-1} \left(\frac{r}{a} \right)^{-3/2}, \quad (12)$$

where $n(r)$ is the density in units of cm^{-3} , r is the distance from the

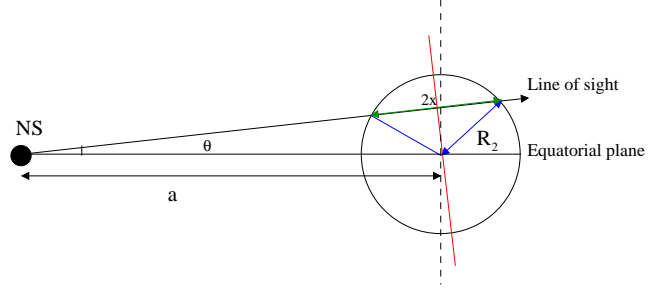


Figure 5. Schematic geometry of MXB 1659-298 not in scale.

inner Lagrangian point, ζ is a parameter that takes into account a non-spherical distribution of matter, η a parameter larger than 1 and \dot{m}_E is the mass transfer rate in units of Eddington mass accretion rate. Adopting a mass transfer rate of $\dot{m} \approx 1.1 \times 10^{-9} M_\odot \text{ yr}^{-1}$, an orbital period of 7.116 hr, a companion star mass and a neutron star mass of $0.76 M_\odot$ and $1.4 M_\odot$, respectively, we obtain that $n(a) \approx 3.3 \times 10^9 (\zeta \eta)^{-1} \text{ cm}^{-3}$. Supposing a constant particle density along the line of sight, we can determine the equivalent hydrogen column density N associated with the neutral matter using $N = n(a) \times a$, where $a \approx 1.7 \times 10^{11} \text{ cm}$ for MXB 1659-298. We find that $N \approx 5.5 \times 10^{20} (\zeta \eta)^{-1} \text{ cm}^{-2}$. Since the quantity $\zeta \eta$ is close the unity (see Iaria et al. 2013) we find that the equivalent hydrogen column of the cold matter is $N \approx 5.5 \times 10^{20} \text{ cm}^{-2}$, that is of the same order of magnitude of the changes observed during quiescence of the source.

The adopted scenario assumes that the mass transfer rate is $\dot{M}_2 \approx -1.1 \times 10^{-9} M_\odot \text{ yr}^{-1}$ (both in outburst and in quiescence) and that the companion star mass is $0.76 M_\odot$; the time scale associated with the mass transfer rate, $\tau_{\dot{M}} = M_2 / |\dot{M}_2|$, is $7 \times 10^8 \text{ yr}$. The companion star is in thermal equilibrium if $\tau_{\dot{M}}$ is longer than the thermal time scale $\tau_{KH} = GM_2^2 / (R_2 L_2)$ of the companion star (Paczynski 1971). To estimate the thermal timescale we need to know the luminosity L_2 of the companion star. For a star close to the lower main sequence it holds the relation $L_2 / L_\odot = (M_2 / M_\odot)^4$ (see Salaris & Cassisi 2005), hence $\tau_{KH} \sim 3.2 \times 10^7 m_2^{-2.88} \text{ yr}$. Since the companion star mass is $0.76 M_\odot$ we obtain that $\tau_{KH} \sim 7.0 \times 10^7 \text{ yr}$ which is one order of magnitude shorter than $\tau_{\dot{M}}$, hence the companion star is in thermal equilibrium.

Assuming a neutron star mass of $1.4 M_\odot$ and a companion star mass of $0.76 M_\odot$ we infer that the Roche lobe radius, R_{L1} of the compact object is $5.5 \times 10^{10} \text{ cm}$. The radius of the accretion disc, R_d , corresponds to the tidal radius R_T that is $R_T \approx 0.9 R_{L1}$ (see Frank et al. 2002, eq. 5.122), hence the accretion disc radius is $R_d \approx 5 \times 10^{10} \text{ cm}$.

Considering that $\Delta T_{ing} \approx 17 \text{ s}$ we can estimate the size of the corona, R_c , surrounding the central source using the relation

$$\frac{2\pi}{P} a = \frac{2R_c}{\Delta T_{ing}} \quad (13)$$

we find that $R_c \approx 3.5 \times 10^8 \text{ cm}$. This result suggests the presence of a compact corona around the neutron star.

We estimate the inclination angle, $i = 90^\circ - \theta$, of the system finding the angle θ shown in Fig. 5. Knowing that the eclipse duration is $\Delta T_{ecl} \approx 899.1 \text{ s}$ we can estimate the length x using

$$\frac{2\pi}{P} a = \frac{2x}{\Delta T_{ecl}}. \quad (14)$$

We obtain that $x \approx 1.9 \times 10^{10} \text{ cm}$, where $2x$ is the green segment shown in Fig. 5. The angle θ , that is the angle between the line of

sight and the equatorial plane of MXB 1659-298, is obtained from

$$\tan \theta = \left[\frac{R_2^2 - x^2}{a^2 - (R_2^2 - x^2)} \right]^{1/2}.$$

We infer that $i \simeq 72^\circ.4$. Our result is compatible with the presence in the light curve of the source of dips and total eclipses that can be observed for inclination angles between 75° and 80° (see Fig. 5.10 in Frank et al. 2002).

Sidoli et al. (2001) detected in the XMM spectrum of MXB 1659-298 the presence of absorption lines associated with the presence of O VIII, Ne IX, Fe XXV and Fe XXVI ions. The authors, assuming an inclination angle of 80° inferred the distance of the absorbing plasma from the central source, finding $r_{\text{Fe}} \lesssim 2.4 \times 10^8$ cm, $r_O \gtrsim 3 \times 10^8$ cm and $r_{\text{Ne}} \gtrsim 9 \times 10^7$ cm, respectively. Revisiting the results obtained by Sidoli et al. (2001) for an inclination angle of $72^\circ.4$ we find $r_{\text{Fe}} \lesssim 8 \times 10^8$ cm, $r_O \gtrsim 1 \times 10^9$ cm and $r_{\text{Ne}} \gtrsim 3 \times 10^8$ cm. Since we have estimated that the size of the corona is $R_c \simeq 3.5 \times 10^8$ cm we suggest that the absorbing plasma is located the outer region of the corona.

Our ephemeris of MXB 1659-298 also include a sinusoidal modulation with a period of 2.31 ± 0.02 yr. This periodic modulation observed in the delays could be produced by the gravitation coupling of the orbit with changes in the shape of the magnetically active companion star. These changes are thought to be the consequence of the torque applied by the magnetic activity of a sub-surface magnetic field in the companion star with convective envelope. The convective envelope induces a cyclic exchange of angular momentum between the inner and outer regions of the companion star causing a change in the gravitational quadrupole moment (see Applegate 1992; Applegate & Shaham 1994). A similar mechanism has been proposed for the eclipsing LMXBs EXO 0748-676 (Wolff et al. 2009) and AX J1745.6-2901 (Ponti et al. 2017).

The periodicity is 843 d and the amplitude is 9.6 s. In this case we find that $\Delta P/P = (8.3 \pm 0.5) \times 10^{-7}$. We estimate that the transfer of angular momentum needed to produce an orbital period change ΔP is $\Delta J \simeq 3.1 \times 10^{46}$ g cm² s⁻¹ (see Applegate 1992, eq. 27). The quantity $\Delta\Omega/\Omega$ is 4.2×10^{-4} , where Ω is the orbital angular velocity of the binary system and $\Delta\Omega$ is the variation of the orbital angular velocity needed to produce ΔP (see Applegate & Shaham 1994, eq. 3). The variable part of the luminosity of the companion star is $\Delta L \simeq 1.4 \times 10^{32}$ erg s⁻¹. Considering that $L_2/L_\odot = (M_2/M_\odot)^4$ we obtain that $L_2 = 0.33 L_\odot$ and, hence, $\Delta L/L_2 \simeq 0.11$, that agrees with the prediction of $\Delta L \simeq 0.1 L$ obtained for magnetic active stars (see Applegate 1992, and references therein). Our results suggest that a change in the magnetic quadrupole of the companion star can produce the observed sinusoidal modulation. The required energy to transfer the angular momentum from the interior of the companion star to a thin shell, with a mass of 10% of M_2 , at the surface (and viceversa) is furnished by ten percentage of the thermonuclear energy produced by the companion star. Furthermore, we obtain that the mean sub-surface magnetic field B of the companion star is close to 1×10^5 G (see Applegate 1992, eq. 23).

The origin of the sinusoidal modulation could also be explained by the presence of a third body orbiting around the binary system, similarly to what is found for the Low-Mass X-ray binary system XB 1916-053 by Iaria et al. (2015). Adopting the inclination angle $i \sim 72^\circ.4$ we find that the orbital separation between the center of mass of MXB 1659-298 and the third body is $a_x \sin i = A c$, where c is the speed of light. Using the values in the third column of Tab. 2 we obtain the $a_x \sin i = (2.9 \pm 0.2) \times 10^{11}$ cm. Assuming a non-eccentric and coplanar orbit of the third body, the mass M_3

of the third body is obtained from

$$\frac{M_3 \sin i}{(M_3 + M_{\text{bin}})^{2/3}} = \left(\frac{4\pi^2}{G} \right)^{1/3} \frac{a_x}{P_{\text{mod}}^{2/3}}, \quad (15)$$

where M_{bin} is the mass of the binary system and P_{mod} is the revolution period of the third body around the binary system (see e.g. Bozzo et al. 2007). We obtain that the mass of the third body is $M_3 = 0.0205 \pm 0.0015 M_\odot$ (corresponding to $21 \pm 2 M_J$).

To verify if a similar hierarchical triple system is stable we adopt the criteria shown by Kiseleva et al. (1994). Since $M_1 = 1.4 M_\odot$, $M_2 = 0.76 M_\odot$ and $M_3 = 0.020 M_\odot$, we define $\alpha = \log_{10}(M_1/M_2)$ and $\beta = \log_{10}[(M_1 + M_2)/M_3]$ finding $\alpha \simeq 0.27$ and $\beta \simeq 2.0$. Furthermore, we define the ratio of the orbital period of the third body with respect to the orbital period of the binary system as $X_0 = P_{\text{mod}}/P \simeq 2840$. Using the obtained values of α and β we find that X_0^{min} is between 3.38 and 3.42 and $X_{\text{SZ}} - X_0^{\text{min}}$ is between 0.48 and 0.68 (Kiseleva et al. 1994, Tabs. 1 and 2). This implies that $X_0 > X_{\text{SZ}}$ therefore the Hill-type stability is verified, i.e. the analysis predicts that orbital exchanges are not possible. Moreover, since $X_{\text{SZ}} - X_0^{\text{min}} > 0$ the system persists indefinitely preserving the same hierarchical ordering.

5 CONCLUSIONS

We have estimated 51 eclipse arrival times of MXB 1659-298 when the source was in outbursts in 2000, 2001 and 2015 using *Ross-XTE*, *XMM-Newton*, *NuSTAR* and *Swift/XRT* data. Adding these times to the previous reported in literature we obtain a baseline of 40 years, from 1976 to 2017, to constrain the ephemeris of the source. The data are clustered in three temporal intervals covering six years corresponding to the periods in which source was in outbursts. We estimate that the companion star mass is $0.76 M_\odot$, in agreement with the possibility that the companion is a early K-type main-sequence star as reported in literature.

Using the RXTE/PCA data we have studied the profile of the total eclipse observing jitters in the ingress/egress duration and eclipse duration of about 10-15 s. The average values of the ingress, egress and eclipse durations are 17.0 ± 0.7 s, 16.7 ± 0.9 s and 899.1 ± 0.6 s, respectively. Using the average ingress and eclipse duration values we find that the size of the corona surrounding the neutron star is $R_c \sim 3.5 \times 10^8$ cm and the inclination angle of the binary system is $\sim 72^\circ.4$.

We find that the eclipse arrival times are well predicted by ephemeris composed of a linear, a quadratic and a sinusoidal term. We find an orbital period derivative of $\dot{P} = -8.5(1.2) \times 10^{-12}$ s s⁻¹. We are able to explain the value of \dot{P} assuming that the mass transfer rate corresponds to the mass accretion rate observed at the peak of the outbursts ($\simeq 1.1 \times 10^{-9} M_\odot \text{ yr}^{-1}$) both during the outbursts and quiescence and assuming that during the outbursts the mass transfer is conservative, while, during quiescence, the mass transfer is totally non-conservative and the matter is ejected from the inner Lagrangian point of the binary system according to the mechanism named *radio ejection* (Burderi et al. 2001).

The sinusoidal modulation has a period of 2.31 ± 0.02 yr and an amplitude of 9.6 ± 0.6 s. This term significantly improves the fit of the delays associated with the eclipse arrival times. The 2.3-yr periodic modulation of the orbital period can be explained either with the presence of a gravitational quadrupole coupling of the orbit or with the presence of a third body orbiting around the binary system. In the second scenario we find that the mass of the third body is $21 \pm 2 M_J$.

Finally, we note that the first two eclipse arrival times, measured during the outburst occurred in 1976-1978, are marginally predicted by the quadratic ephemeris. To fit them we adopted a more complex ephemeris taking into account the second derivative of the orbital period. However, the statistical improvement is smaller than three σ . A larger baseline is needed to confirm or discard more complex ephemeris.

ACKNOWLEDGEMENTS

This research has made use of data and/or software provided by the High Energy Astrophysics Science Archive Research Center (HEASARC), which is a service of the Astrophysics Science Division at NASA/GSFC and the High Energy Astrophysics Division of the Smithsonian Astrophysical Observatory. This research has made use of MAXI data provided by RIKEN, JAXA and the MAXI team. We are grateful to the *Swift* team, and especially Kim Page, for their assistance and flexibility in the scheduling of our ToO observations. We acknowledge the use of public data from the *Swift* data archive. This work was partially supported by the Regione Autonoma della Sardegna through POR-FSE Sardegna 2007-2013, L.R. 7/2007, Progetti di Ricerca di Base e Orientata, Project N. CRP-60529. We also acknowledge a financial contribution from the agreement ASI-INAF I/037/12/0. AR and AS gratefully acknowledge the Sardinia Regional Government for its financial support (P.O.R. Sardegna F.S.E. Operational Programme of the Autonomous Region of Sardinia, European Social Fund 2007-2013 - Axis IV Human Resources, Objective 1.3, Line of Activity 1.3.1.). We also acknowledge fruitful discussions with the international team on "The disk magnetosphere interaction around transitional ms pulsars" supported by ISSI (International Space Science Institute), Bern".

REFERENCES

Applegate J. H., 1992, *ApJ*, **385**, 621
 Applegate J. H., Shaham J., 1994, *ApJ*, **436**, 312
 Bahramian A., Heinke C. O., Wijnands R., Degenaar N., 2016, The Astronomer's Telegram, **8699**
 Bozzo E., et al., 2007, *A&A*, **476**, 301
 Burderi L., et al., 2001, *ApJ*, **560**, L71
 Burderi L., Riggio A., di Salvo T., Papitto A., Menna M. T., D'Ai A., Iaria R., 2009, *A&A*, **496**, L17
 Burderi L., Di Salvo T., Riggio A., Papitto A., Iaria R., D'Ai A., Menna M. T., 2010, *A&A*, **515**, A44
 Burrows D. N., et al., 2005, *Space Sci. Rev.*, **120**, 165
 Cackett E. M., Wijnands R., Miller J. M., Brown E. F., Degenaar N., 2008, *ApJ*, **687**, L87
 Cackett E. M., Brown E. F., Cumming A., Degenaar N., Fridriksson J. K., Homan J., Miller J. M., Wijnands R., 2013, *ApJ*, **774**, 131
 Chou Y., 2014, *Research in Astronomy and Astrophysics*, **14**, 1367
 Claret A., Gimenez A., 1989, *A&AS*, **81**, 37
 Cominsky L. R., Wood K. S., 1984, *ApJ*, **283**, 765
 Cominsky L. R., Wood K. S., 1989, *ApJ*, **337**, 485
 Cominsky L., Ossmann W., Lewin W. H. G., 1983, *ApJ*, **270**, 226
 Di Salvo T., Burderi L., Riggio A., Papitto A., Menna M. T., 2008, *MNRAS*, **389**, 1851
 Díaz Trigo M., Parmar A. N., Boirin L., Méndez M., Kaastra J. S., 2006, *A&A*, **445**, 179
 Filippenko A. V., Leonard D. C., Matheson T., Li W., Moran E. C., Riess A. G., 1999, *PASP*, **111**, 969
 Frank J., King A., Raine D. J., 2002, *Accretion Power in Astrophysics: Third Edition*

Galloway D. K., Muno M. P., Hartman J. M., Psaltis D., Chakrabarty D., 2008, *ApJS*, **179**, 360
 Gehrels N., et al., 2004, *ApJ*, **611**, 1005
 Harrison F. A., et al., 2013, *ApJ*, **770**, 103
 Iaria R., Di Salvo T., D'Ai A., Burderi L., Mineo T., Riggio A., Papitto A., Robba N. R., 2013, *A&A*, **549**, A33
 Iaria R., et al., 2015, *A&A*, **582**, A32
 Jahoda K., Swank J. H., Giles A. B., Stark M. J., Strohmayer T., Zhang W., Morgan E. H., 1996, in Siegmund O. H., Gummin M. A., eds, *Proc. SPIE Vol. 2808, EUV, X-Ray, and Gamma-Ray Instrumentation for Astronomy VII*. pp 59–70, doi:10.1117/12.256034
 Jansen F., et al., 2001, *A&A*, **365**, L1
 Kiseleva L. G., Eggleton P. P., Orlov V. V., 1994, *MNRAS*, **270**, 936
 Levine A. M., Bradt H., Cui W., Jernigan J. G., Morgan E. H., Remillard R., Shirey R. E., Smith D. A., 1996, *ApJ*, **469**, L33
 Lewin W. H. G., Hoffman J. A., Doty J., Liller W., 1976, *IAU Circ.*, **2994**
 Matsuoka M., et al., 2009, *PASJ*, **61**, 999
 Mihara T., et al., 2011, *PASJ*, **63**, S623
 Negoro H., et al., 2015, The Astronomer's Telegram, **7943**
 Oosterbroek T., Parmar A. N., Sidoli L., in't Zand J. J. M., Heise J., 2001, *A&A*, **376**, 532
 Paczyński B., 1971, *ARA&A*, **9**, 183
 Patterson J., 1984, *ApJS*, **54**, 443
 Ponti G., De K., Muñoz-Darias T., Stella L., Nandra K., 2017, *MNRAS*, **464**, 840
 Salaris M., Cassisi S., 2005, *Evolution of Stars and Stellar Populations*
 Sanna A., et al., 2016, *MNRAS*, **459**, 1340
 Sidoli L., Oosterbroek T., Parmar A. N., Lumb D., Erd C., 2001, *A&A*, **379**, 540
 Smith M. A., 1979, *PASP*, **91**, 737
 Strüder L., et al., 2001, *A&A*, **365**, L18
 Verbunt F., 2001, *A&A*, **368**, 137
 Wachter S., Smale A. P., Bailyn C., 2000, *ApJ*, **534**, 367
 Warner B., 1995, *Cataclysmic Variable Stars*. Cambridge Astrophysics, Cambridge University Press
 Wijnands R., Strohmayer T., Franco L. M., 2001, *ApJ*, **549**, L71
 Wijnands R., Nowak M., Miller J. M., Homan J., Wachter S., Lewin W. H. G., 2003, *ApJ*, **594**, 952
 Wolff M. T., Hertz P., Wood K. S., Ray P. S., Bandyopadhyay R. M., 2002, *ApJ*, **575**, 384
 Wolff M. T., Wood K. S., Ray P. S., 2007, *ApJ*, **668**, L151
 Wolff M. T., Ray P. S., Wood K. S., Hertz P. L., 2009, *ApJS*, **183**, 156
 in 't Zand J., Heise J., Smith M. J. S., Cocchi M., Natalucci L., Celidonio G., Augusteijn T., Freyhammer L., 1999, *IAU Circ.*, **7138**

This paper has been typeset from a \LaTeX file prepared by the author.